A Functional Link between Dynamin and the Actin Cytoskeleton at Podosomes

Gian-Carlo Ochoa,*‡ Vladimir I. Slepnev,*‡ Lynn Neff,‡§ Niels Ringstad,*‡ Kohji Takei,*‡ Laurie Daniell,*‡ Warren Kim,*‡ Hong Cao,‖ Mark McNiven,‖ Roland Baron,‡§ and Pietro De Camilli*‡

*Howard Hughes Medical Institute, ‡Department of Cell Biology and §Department of Orthopaedic Surgery, Yale University School of Medicine, New Haven, Connecticut 06510; and ‖Mayo Clinic, Rochester, Minnesota 55905

Abstract. Cell transformation by Rous sarcoma virus results in a dramatic change of adhesion structures with the substratum. Adhesion plaques are replaced by dot-like attachment sites called podosomes. Podosomes are also found constitutively in motile nontransformed cells such as leukocytes, macrophages, and osteoclasts. They are represented by columnar arrays of actin which are perpendicular to the substratum and contain tubular invaginations of the plasma membrane. Given the similarity of these tubules to those generated by dynamin around a variety of membrane templates, we investigated whether dynamin is present at podosomes. Immunoreactivities for dynamin 2 and for the dynamin 2–binding protein endophilin 2 (SH3P8) were detected at podosomes of transformed cells and osteoclasts. Furthermore, GFP wild-type dynamin 2aa was targeted to podosomes. As shown by fluorescence recovery after photobleaching, GFP-dynamin 2aa and GFP-actin had a very rapid and similar turnover at podosomes. Expression of the GFP-dynamin $2aa^{G273D}$ abolished podosomes while GFP-$dynamin^{K44A}$ was targeted to podosomes but delayed actin turnover. These data demonstrate a functional link between a member of the dynamin family and actin at attachment sites between cells and the substratum.

Key words: clathrin • endocytosis • actin patches • Src • osteoclast

Introduction

Dynamin is a GTPase that plays a critical role in endocytosis. In mammals it occurs as three distinct isoforms (dynamin 1, 2, and 3) with different cellular and subcellular distributions (Urrutia et al., 1997; Schmid et al., 1998). Based on studies of the *Drosophila melanogaster shibire* mutant which harbors a temperature-sensitive mutation in the dynamin gene, dynamin was proposed to mediate the fission of endocytic vesicles from the plasma membrane in nerve terminals (Koenig and Ikeda, 1989; Chen et al., 1991; van der Bliek and Meyerowitz, 1991). Subsequent studies have generalized this putative function of dynamin to clathrin-mediated endocytosis in all cells (Herskovits et al., 1993; van der Bliek et al., 1993) and more recently to other forms of endocytosis (Schnitzer et al., 1996; Henley et al., 1998; Gold et al., 1999). Ultrastructural analysis of nerve terminals of *shibire* mutants after exposure to the restrictive temperature (Koenig and Ikeda, 1983) and of membrane templates incubated with brain cytosol, ATP and GTPγS (Takei et al., 1995), have shown that dynamin can oligomerize into rings or stacks of rings at the neck of endocytic vesicles, consistent with its putative role in the separation of endocytic vesicles from the plasma membrane. Stacks of rings produce in peculiar elongations of the neck of endocytic pits into narrow tubules (Takei et al., 1995).

The precise mechanism of action of dynamin in the pinching-off reaction of endocytic vesicles remains unclear and several models have been proposed. While some models suggest that dynamin acts as a mechanochemical enzyme which severs the vesicle stalk (Hinshaw and Schmid, 1995; Takei et al., 1995; Sweitzer and Hinshaw, 1998), other models propose that dynamin acts indirectly by recruiting or regulating downstream effectors (De Camilli and Takei, 1996; Roos and Kelly, 1997). The latter possibility has recently been supported by the report that GTP hydrolysis by dynamin may not be required for the endocytic reaction (Sever et al., 1999).

Although the majority of studies implicate dynamin in endocytosis, there is evidence to suggest that this GTPase may play additional functions in cell physiology. Dynamin alone, or dynamin in combination with amphiphysin, was shown to evaginate lipid membranes into tubules with a diameter very similar to that of collars of deeply invaginated clathrin-coated pits (Sweitzer and Hinshaw, 1998; Takei et al., 1998, 1999). This finding indicates that membrane tubulation by dynamin does not require a coated endocytic pit as a template, and hints to a possible role of dynamin in membrane dynamics independent of an en-

Address correspondence to Pietro De Camilli, Department of Cell Biology, Yale University School of Medicine, 295 Congress Avenue, New Haven, CT 06510. Tel.: (203) 737-4465. Fax: (203) 737-4436. E-mail: pietro.decamilli@yale.edu

docytic vesicle bud. In growth cones, dynamin colocalizes with actin, and disruption of the function of either dynamin or the dynamin-binding protein amphiphysin impairs growth cone dynamics (Torre et al., 1994; Mundigl et al., 1998). Dynamin also binds profilin II (Witke et al., 1998), a major regulator of the actin based cytoskeleton, as well as syndapin/pacsin/FAP52 (Merilainen et al., 1997; Qualmann et al., 1999; Ritter et al., 1999), a protein implicated in the attachment of the actin cytoskeleton to membranes. Many studies have implicated actin in endocytosis (Munn et al., 1995; Lamaze et al., 1997; Wendland and Emr, 1998; Merrifield et al., 1999). Thus, one potential downstream effector of dynamin may be the actin cytoskeleton and effects of dynamin on actin may underlie its role both in endocytosis and in other cellular functions.

The proline-rich COOH terminus of dynamin was shown to interact with a variety of SH3 domain containing proteins including Src (Gout et al., 1993) a non-receptor tyrosine kinase that plays a key role in actin-mediated cell adhesion and motility (Thomas and Brugge, 1997). Previous studies have shown that activated forms of Src induce a profound change in attachment structures between the cell and the substratum (Tarone et al., 1985). Focal adhesions are replaced by dot-like contacts sites, called podosomes (Tarone et al., 1985; Marchisio et al., 1988; Nitsch et al., 1989) which are columnar arrays of actin cytoskeleton often containing a narrow tubular invagination of the plasmalemma roughly perpendicular to the substratum. In some cells, podosomes cluster in a peculiar rosette-like arrangement (Nitsch et al., 1989). Podosomes are constitutively found in osteoclasts (Zambonin-Zallone et al., 1988) where Src plays an essential role (Soriano et al., 1991; Tanaka et al., 1996). In these cells podosomes are arranged in a ring at the cell periphery where they mediate the attachment and motility of the osteoclast on bone and generate the sealed compartment where bone resorption takes place (Zambonin-Zallone et al., 1988; Tanaka et al., 1996). Furthermore, podosomes are present in leukocytes and macrophages where they play a role in migration and diapedesis (Wolosewick, 1984; DeFife et al., 1999; Linder et al., 1999). The membrane tubules which represent the core of podosomes are very similar in diameter to tubules generated by the oligomerization of dynamin around membrane templates (Takei et al., 1995, 1998; Sweitzer and Hinshaw, 1998). Prompted by this similarity, and by the potential connection of dynamin both to actin function and to Src, we investigated whether dynamin is concentrated at podosomes.

Materials and Methods

Antibodies and Reagents

Monoclonal antibodies directed against dynamin (Hudy-1 and D25520), vinculin and actin were purchased from Upstate Biotechnology, Transduction Laboratories, Boehringer, and ICN Biomedicals, respectively. Rabbit polyclonal antibodies specifically directed against endophilin 2 were raised using a peptide corresponding to sequence unique to rat endophilin 2 (SH3P8) within the region of the protein which differs among endophilin 1, 2 and 3, also called SH3P4, SH3P8, and SH3P13 (Ringstad et al., 1997). Rabbit pan-endophilin antibodies (serum 2 of Ringstad et al., 1997), rabbit anti-dynamin-2 polyclonal antibodies (Dyn2; Cao et al., 1998) and a monoclonal anti-Src antibody (#327; Horne et al., 1992) were previously described. Monoclonal antibodies directed against clathrin's heavy chain (X-22) and cortactin were kind gifts of Dr. Francis Brodsky (University of California) and Dr. J. Thomas Parsons (University of Virginia), respectively. Rhodamine and fluorescein-labeled phalloidin was purchased from Molecular Probes. Secondary antibodies conjugated with CY3 and Oregon Green were purchased from Jackson Immunochemicals and Molecular Probes, respectively. Cyclosporin A was purchased from Calbiochem-Novabiochem.

Cell Culture and Immunocytochemistry

BHK21 and RSV-transformed BHK21 cells were cultured at 37°C in GMEM, 10% (vol/vol) Tryptose Phosphate Broth, 10% (vol/vol) FBS, and 100 U/ml each of penicillin and streptomycin. Before fixation, RSV-transformed BHK21 cells were grown in 2% FBS for 12 h and then for additional two hours in 0.2% FBS. BHK21 cells were transfected using LipofectAMINE Plus (GIBCO BRL) reagent according to the manufacturer's protocol.

Cells were fixed in 4% formaldehyde (freshly prepared from paraformaldehyde) in 0.1 M phosphate buffer, detergent-permeabilized, immunostained and prepared for microscopic observation as previously described (Cameron et al., 1991). Cells were visualized using a Zeiss Axiophot 2.

cDNAs

In this manuscript the term dynamin 2aa (rat) applies to the Genebank sequence #B53165. This sequence was previously referred to as either dynamin 2aa (Cao et al., 1998) or dynamin 2ba (Sontag et al., 1994) by different groups. Constructs encoding GFP-dynamin 2aa (COOH-terminal–linked GFP) were previously described (Cao et al., 1998). GFP-dynamin $2aa^{G273D}$ and GFP-dynamin $2aa^{K44A}$ were generated by a modified Stratagene "QuickChange" site-directed mutagenesis technique following manufacturer's instructions. The Pfu DNA polymerase was replaced by Pwo DNA polymerase (Roche) for initial amplification reaction. Mutations were verified by sequencing. A construct encoding GFP-actin (NH_2-terminal GFP linked by 5 glycines to chicken β-actin in a CMV driven vector) was a kind gift of Dr. Michael Way (EMBL, Heidelberg).

Electron Microscopy

RSV-transformed BHK21 cells and osteoclasts were washed with phosphate buffered saline (PBS) at 37°C, then fixed in 1.5% glutaraldehyde in 0.1 M Na-Cacodylate, and postfixed with 1% OsO_4 and 1.5% K_3FeCN_6 in 0.1 M Na-Cacodylate. En bloc staining with 0.4% uranyl acetate (Mg) was performed before Epon embedding by standard procedures. Cell-free incubations of brain membranes with brain cytosol, ATP and GTPγS and immunolabeling of these preparations for dynamin and actin were performed as described (Takei et al., 1995).

Immunoprecipitation and Affinity Chromatography

RSV-transformed BHK21 cells were washed with 120 mM phosphate buffer pH 7.4, and removed with a cell scraper (Becton Dickinson) in the presence of 10 mM Hepes, 150 mM NaCl, and 1% Triton X-100. The extract was then centrifuged for 10 minutes at 14,000 rpm in an Eppendorf centrifuge. 200 μg of extract was incubated with 2 μg of affinity-purified antibodies for 1 h at 4°C. Immune complexes were precipitated with 50 ml of protein A–Sepharose, extensively washed with 10 mM Hepes/150 mM NaCl, and eluted in 200 μl of SDS/PAGE sample buffer. Conditions for affinity-chromatography on the GST fusion protein of the SH3 domain of endophilin 2 were previously described (Ringstad et al., 1997).

Isolation and Preparation of Osteoclasts

Mouse osteoclasts were isolated according to procedures previously described (Chambers and Magnus, 1982; Ali et al., 1984). In brief, long bones from 14–21-d-old mice were dissected free of adherent tissue and placed in α-MEM containing 10% FBS. They were minced into small pieces and pipetted vigorously to release osteoclasts. Bone particles were then allowed to sediment for 30 s and the remaining suspension containing osteoclasts was seeded onto serum coated coverslips. Coverslips were incubated 18–24 h at 37°C to allow cell attachment. Cells on coverslips were then fixed with 3.7% formaldehyde in PBS for 10 min at room temperature, washed in PBS and processed for double immunofluorescence as de-

scribed above for BHK21 cells. In some experiments cells were treated with cyclosporin A (20 μM) for 20 min before fixation.

Microinjection of Osteoclasts

cDNA constructs were microinjected using an Eppendorf 5246 microinjector with Femtotip needles. During injection osteoclasts were maintained in α-MEM, 10% FBS and 1 mM Hepes. After injection they were returned to the α-MEM media lacking Hepes and left to grow at 37°C for 6 h before fixation and immunostaining.

Fluorescence Recovery after Photobleaching

Fluorescence recovery after photobleaching (FRAP)[1] experiments were conducted on a BioRad MRC 1024 two photon scanning laser microscope equipped with a krypton/argon laser and a sapphire Ti laser. The krypton/argon laser was used to excite the GFP-tagged proteins at 488 nm and emissions above 515 nm were collected. In each experiment, at least 20 consecutive baseline images were obtained. Then a region in the podosome rosette was selected and photobleached using the sapphire Ti laser at 920 nm for 20 s at 50% power. After photobleaching, fluorescence of the entire field was collected by the krypton/argon laser at 3% power every second for at least 1 min after bleaching. The fluorescence intensity in the photobleached region of the podosome rosette at various times of recovery was normalized to the fluorescence intensity measured in a nonbleached region of the same rosette at the same post-bleaching time. This procedure allowed to account for the decreased fluorescence due to overall bleaching of the entire field. The fluorescence recovery curve was $F(t) = F_{ss}(1-e^{-kt})+F_0$ where F(t) is the fluorescence in the bleached area at time t, F_{ss} is the net amount of fluorescence recovered at steady state, F_0 is the fluorescence in the bleached area immediately after photobleaching, and k is the constant that describes the rate of fluorescence recovery. Statistical analysis was performed with all values given as a means of at least 6 sets of measurements ± SEM. A *t* test was performed to compare the rate constants of the various curves and a *P* value of <0.05 was taken as significant. Nonlinear regression and *t* tests were performed using Microsoft Excel 4.0.

[1]*Abbreviation used in this paper:* FRAP, fluorescence recovery after photobleaching.

Results

Presence of Dynamin 2aa at Podosomes of Rous Sarcoma Virus-transformed BHK21 Cells

Rous sarcoma virus (RSV)-transformed BHK21 cells were stained with a variety of antibodies which recognize one or more of the three main dynamin isoforms, dynamin 1, 2, and 3. In these BHK21 cells, podosomes cluster in a typical rosette-like arrangement which can be visualized at the light microscopic level by staining for filamentous actin (Fig. 1, B and D) and for other podosome markers such as vinculin and talin (Fig. 1 A and data not shown; Marchisio et al., 1988). Electron micrographs of the rosette in sections cut perpendicular and parallel to the substratum demonstrate the characteristic juxtaposition of individual podosomes, i.e., of columns of actin cytoskeleton surrounding a central membrane tubule (Fig. 2 A–D; Nitsch et al., 1989). As shown in sections perpendicular to the sub-

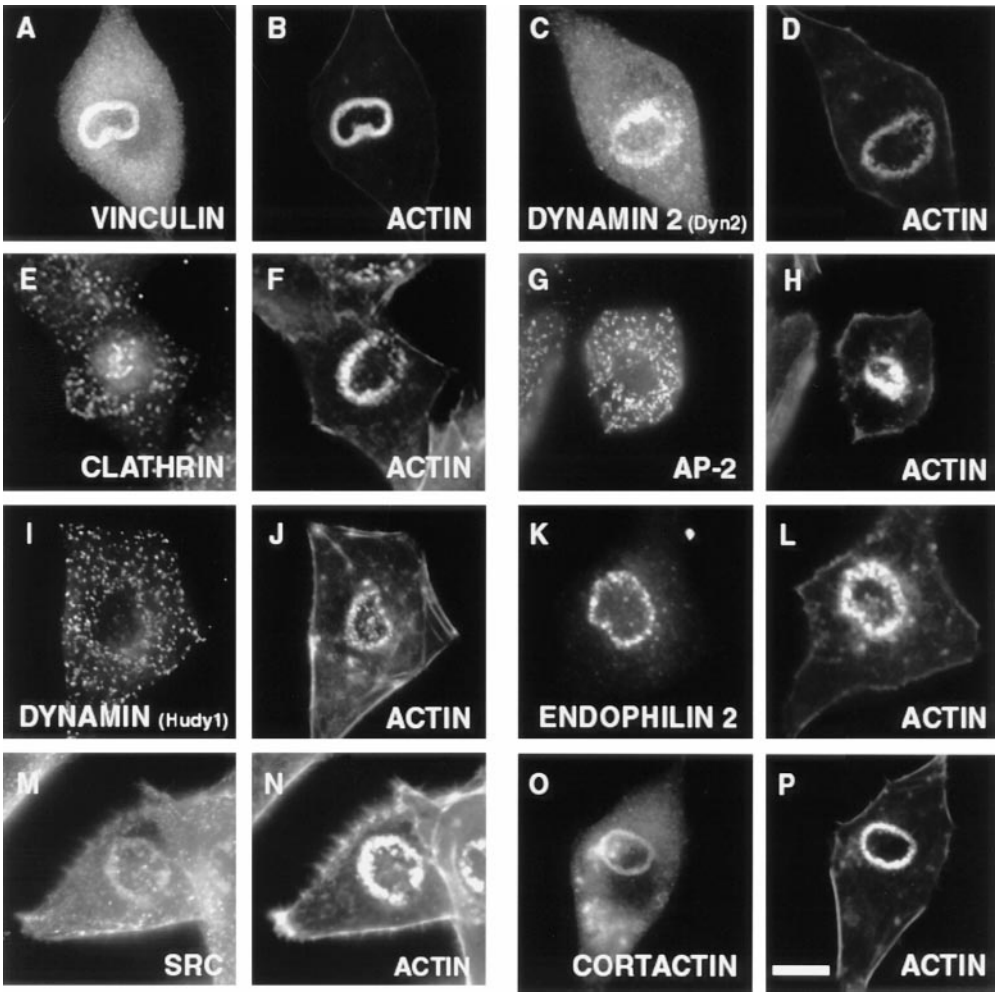

Figure 1. Colocalization of dynamin 2 and endophilin 2 with a variety of podosomal markers and with filamentous actin in podosomes rosettes of RSV-transformed BHK21 cells. Serum-starved cells were reacted by immunofluorescence for the proteins indicated and counterstained with phalloidin. Dynamin was labeled with two different antibodies, Dyn2 and Hudy-1, and only Dyn 2 labels podosomes. Bar, 14 μM.

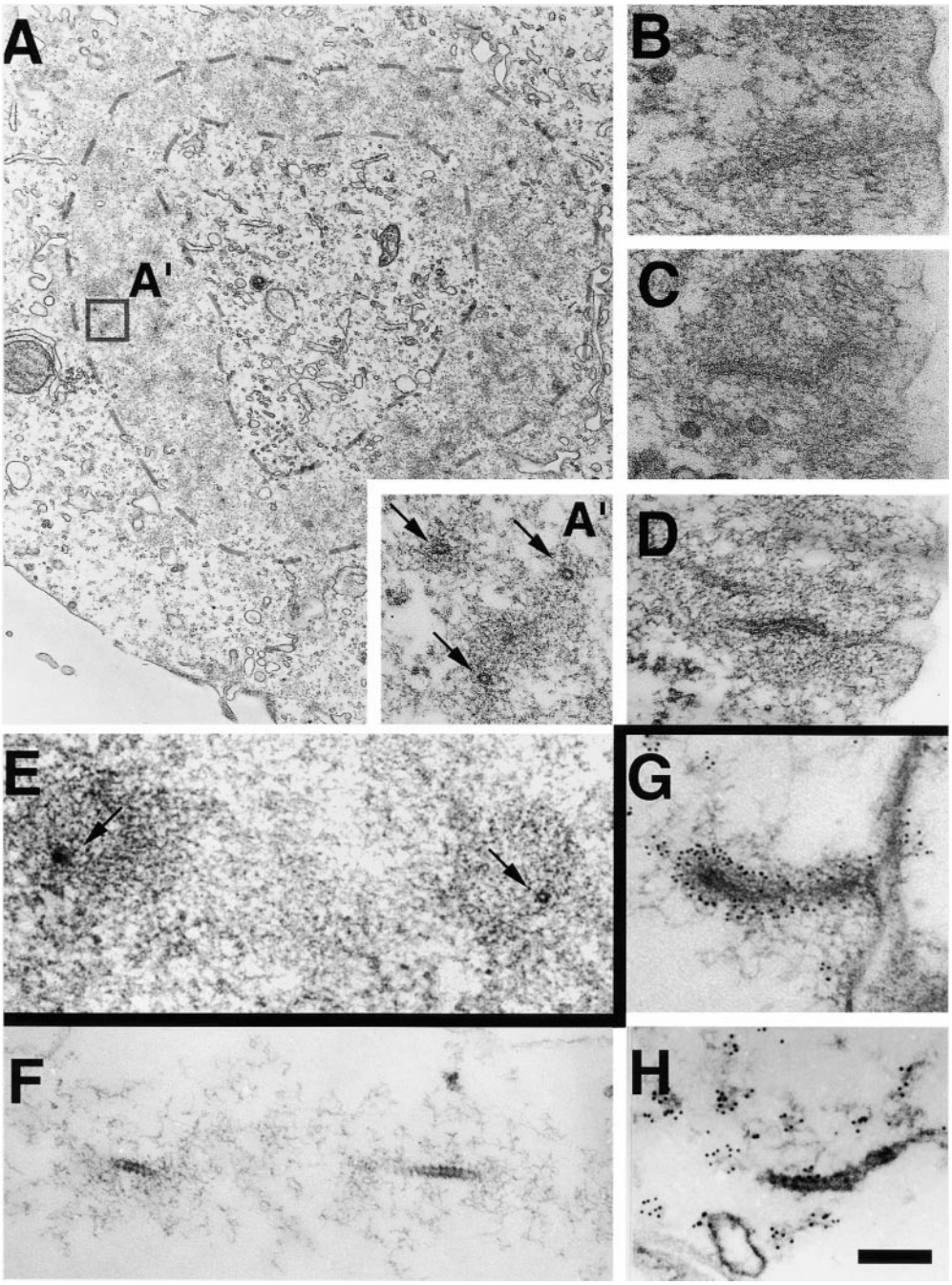

Figure 2. Comparative electron micrographs of tubular membrane invaginations surrounded by an actin sheath at podosomes and in synaptic membrane preparations incubated in cell-free conditions. (A) RVS-transformed BHK21 cell cut parallel to the substratum demonstrating an actin-rich ring (dashed lines) which excludes other organelles and which results from the rosette-like apposition of individual podosomes. The presence of a cross-sectioned tubule in the core of each podosomes (arrows) is shown in A′, which represents a high magnification of the regions enclosed by a square. (B–D) High power views of three podosomes from sections of RVS-transformed BHK21 cells cut perpendicular to the substratum and demonstrating the presence of tubular plasma membrane invaginations. (E) High magnification of two podosomes from the peripheral region of a mouse osteoclast grown on a coverslip and cut parallel to the substratum. Arrows point to cross-sectioned tubules. (F–H) Dynamin-coated tubules from synaptic membranes incubated with brain cytosol, ATP, and GTPγS. G and H show immunolabeling for dynamin and actin, respectively. Note the similarity of these structures to podosomes. Bar: (A) 0.6 nm; (A′ and B–H) 200 nM.

stratum, these tubules are continuous with the cell surface (Fig. 2, B–D). Their diameter (~25 nm) is the same as that of dynamin coated tubules observed in synaptic membranes (Takei et al., 1995). Of the several anti-dynamin antibodies tested, the Dyn2 antibody, which was raised against the proline-rich region of human dynamin 2aa (data are available from GenBank/EMBL/DDBJ under accession number B53165; Jones et al., 1998), labeled very intensely podosome rosettes, as revealed by double staining for filamentous actin with phalloidin (Fig. 1, C and D). In homogenates of BHK21 cells this antibody specifically recognized a band with the expected mobility of dynamin 2 (Fig. 3 A). In addition, the Dyn2 antibody specifically depleted BHK21 cell extracts of dynamin 2 immunoreactivity recognized by another anti-dynamin antibody which recognizes dynamin 2 (D25520) (Fig. 3 B). Colocalization of the Dyn2 immunoreactive materials with actin did not occur throughout the cell. The few stress fibers present in these transformed cells were not stained (data not shown), demonstrating a selective association of dynamin with the podosome pool of actin.

Podosomes were not labeled by antibodies directed against either clathrin (Fig. 1, E and F) or the endocytic clathrin adaptor AP-2 (Fig. 1, G and H), thus indicating that podosomes are not a preferential site for clathrin-mediated endocytosis. Similarly, internalized transferrin, which is taken up by receptor-mediated endocytosis, did not show any preferential association with podosome ro-

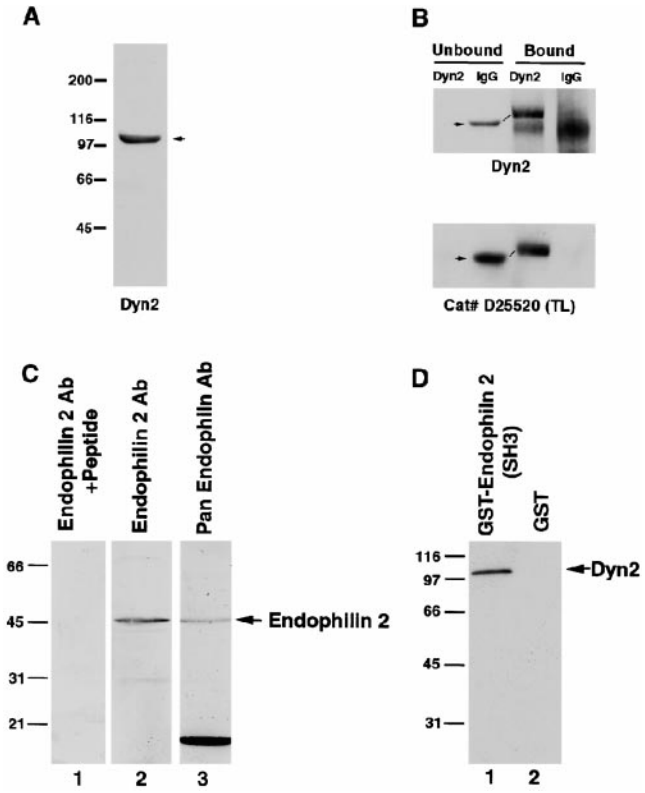

Figure 3. The Dyn2 antibody recognizes selectively dynamin in RSV-transformed BHK21 cell extracts and dynamin 2 specifically interacts with endophilin 2. (A) Western blot of a detergent extract of RSV-transformed BHK21 cells with the Dyn2 antibody. (B) Triton X-100 extracts of RSV-transformed BHK21 cells were immunoprecipitated with Dyn2 antibodies or control IgGs and the immunoprecipitates were reacted by Western blotting with either the Dyn2 antibody (top) or a commercial anti-dynamin antibody (#D25520 from Transduction Laboratories) which recognizes both dynamin 1 and 2. Note that the Dyn2 antibody depletes dynamin immunoreactivity (arrows) from the extract. The slower mobility of dynamin 2 in the bound material was consistently observed and may reflect the absence of Triton X-100 in the load. (C) Extracts of RSV-transformed BHK21 cells extracts were reacted by Western blotting with an endophilin 2-specific antibody in the presence or absence of the peptide used as the immunogen (lanes 1 and 2) or with a pan-endophilin antibody (lane 3). (D) A Triton X-100 extract of RSV-transformed BHK21 cells was incubated with either a GST fusion protein of the SH3 domain of endophilin 2 (lane 1) or GST alone (lane 2). The bound material was then reacted by Western blotting with the Dyn2 antibody.

settes (data not shown). Dynamin immunoreactivity recognized by Hudy-1 antibodies, previously shown to recognize dynamin at clathrin coated pits (Damke et al., 1994), was also not localized at podosomes (Fig. 1, I and J).

Podosomes Are Positive for a Dynamin-binding Protein

Podosomes, however, were intensely and specifically labeled with antibodies directed against endophilin 2 (SH3P8; Fig. 1, K and L) a member of a family of three highly homologous proteins (endophilin 1, 2, and 3, also referred to as SH3P4, SH3P8, and SH3P13) that interact with dynamin via a COOH-terminal SH3 domain (Sparks et al., 1996; Ringstad et al., 1997, 1999; Schmidt et al., 1999). This immunofluorescence pattern was blocked by the presence in the immunostaining solution of the endophilin 2 peptide used as the immunogen for the generation of the antibodies (data not shown). Furthermore, presence of authentic endophilin 2 immunoreactivity in RSV-transformed BHK21 cells was confirmed by Western blot analysis (Fig. 3 C). The anti-endophilin 2 antibody recognized a 45-kD band with the expected mobility of endophilin 2 (Fig. 3 C, lanes 1 and 2) and this band comigrated with a band recognized by an antibody directed against all members of the endophilin family (Fig. 3 C, lane 3). Endophilin 1, 2, and 3 have a pattern of expression which closely mimics that of dynamin 1, 2, and 3, respectively (Ringstad et al., 1997), and recent studies have suggested a functional partnership between dynamin 1 and endophilin 1 (SH3P4; Ringstad et al., 1999; Schmidt et al., 1999). An interaction between dynamin 2 and the SH3 domain of endophilin 2 was demonstrated by the property of a GST fusion protein of this domain to affinity-purify dynamin 2 immunoreactivity from BHK21 cell extracts (Fig. 3 D). Thus, the presence of endophilin 2 at podosomes supports a physiological role for dynamin 2 at these attachment sites. Podosome rosettes are also immunoreactive for Src (Fig. 1, M and N; Gavazzi et al., 1989; Nermut et al., 1991), which bind and phosphorylate dynamin (Gout et al., 1993; Foster-Barber and Bishop, 1998; Ahn et al., 1999) and for cortactin (Fig. 1, O and P) another SH3 domain containing protein (Wu and Parsons, 1993) which binds dynamin in vitro (McNiven, M., unpublished observation).

The rosette-like distribution of dynamin 2 immunoreactivity and of other podosome markers was not observed in non–RSV-transformed BHK21 cells (Fig. 4, A–D), although even in these cells a fraction of Dyn2 immunoreactivity was colocalized with peripheral actin (Fig. 4, C and D). Finally, the localization of Dyn2 immunoreactivity at podosomes was not unique to RSV-transformed BHK21 cells but was also observed in v-Src–transformed Balb 3T3 cells, where podosomes remain isolated and scattered throughout the cell (data not shown).

GFP-dynamin 2aa Is Targeted to Podosomes

Since some antibodies reported to react with dynamin 2 did not label podosomes (not shown), we next searched for more direct evidence demonstrating the property of a dynamin 2 isoform to concentrate at podosomes. RSV-transformed BHK21 cells were transiently transfected with a construct encoding rat GFP-dynamin 2aa (dynamin 2aa; data are available from GenBank/EMBL/DDBJ under accession number B53165). GFP-tagged dynamin 2aa accumulated at podosomes, as shown by the analysis of living cells (Fig. 5 A), or of fixed cells counterstained for actin by phalloidin (Fig. 5, B and C). Individual podosomes were clearly resolved by high power observation of these cells (Fig. 5 A). The lack of reactivity with podosomes of some antibodies which recognize dynamin 2 reflects a selective immunoreactivity of podosomal dynamin. This result may have several explanations including one or more of the following possibilities: alternative splicing, epitope masking,

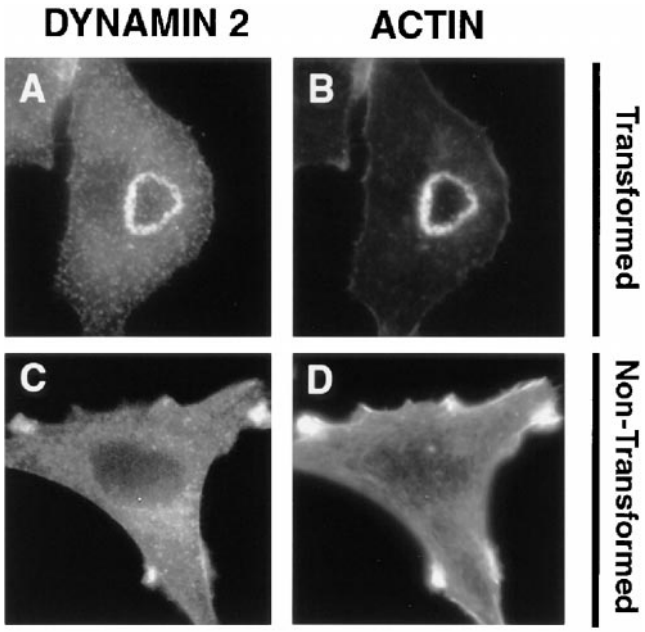

Figure 4. Colocalization of dynamin 2 immunoreactivity and actin in RSV-transformed and nontransformed BHK21 cells. (A–D) RSV-transformed and nontransformed BHK21 cells were stained by immunofluorescence for dynamin 2 with the Dyn2 antibody and for actin with phalloidin. In both cells a partial colocalization of dynamin 2 with actin is observed even though the podosomes rosette is only visible in transformed cells.

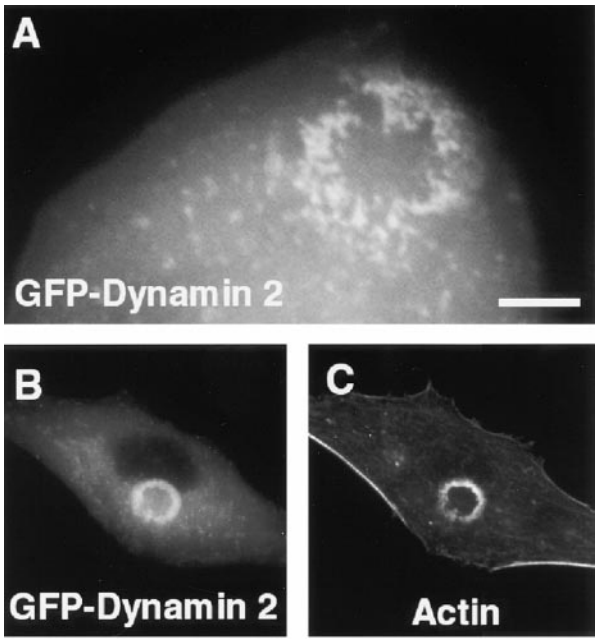

Figure 5. Targeting of transfected dynamin 2aa to podosomes of RSV-transformed BHK21 cells. (A) A RSV-transformed BHK21 cell was transfected with GFP-dynamin 2aa and examined by a CCD camera 12 h after transfected. In this living cell GFP fluorescence reveals individual podosomes. Most, but not all of them, are clustered at the rosette. (B and C) RSV-transformed BHK21 were transformed with GFP-dynamin 2aa, fixed, and then counterstained for actin with phalloidin. Bar: (A) 7 μM; (B and C) 14 μM.

covalent modifications or other forms of posttranslational protein modification.

Dynamin 2 Is Also Present at Podosomes of Osteoclasts

To insure that this localization of dynamin was not a consequence of cell transformation or specific of v-Src expressing cells, we then examined a nontransformed cell known to contain podosomes. In osteoclasts, a peripheral actin-rich ring comprising podosomes, which may be seen as an exaggeration of the podosome rosette present in RSV-transformed BHK21 cells, forms the tight seal with the bone which delimits the compartment of bone resorption (Zambonin-Zallone et al., 1988; Tanaka et al., 1996). A similar podosome-enriched actin ring is formed by osteoclasts when they are cultured in vitro on serum-coated coverslips. Presence of narrow tubular invaginations within these podosomes was confirmed by electron microscopy (Fig. 2 E). When mice osteoclasts cultured on coverslips were immunostained for dynamin 2 and endophilin 2, intense immunoreactivity for both proteins was observed in the peripheral actin-rich ring (Fig. 6, A–D). In addition, after microinjection of DNA encoding GFP-dynamin 2aa, the expressed GFP fusion protein localized predominantly at podosomes (Fig. 6, E and F). Treatment of osteoclasts with cytochalasin B disrupted the peripheral actin ring resulting in a major change in cell morphology and a concomitant redistribution of dynamin 2 immunoreactivity (data not shown).

Disruption of Podosomes by Cyclosporin A

Studies in the nervous system have demonstrated that dynamin 1 is a substrate for the enzymatic activity of the calcium-dependent phosphatase calcineurin (Liu et al., 1994; Bauerfeind et al., 1997). Furthermore Dynamin 1 was shown to bind directly to calcineurin (Lai et al., 1999). Dynamin 1 undergoes constitutive phosphorylation in the nerve terminal and its Ca^{2+}-triggered calcineurin-dependent dephosphorylation is thought to be required for the endocytic reaction (Liu et al., 1994). Dephosphorylation enhances the interaction of dynamin with its binding partners (Slepnev et al., 1998) and decreases its GTPase activity (Liu et al., 1994), thus prolonging the half-life of GTP-dynamin. Accordingly, calcineurin inhibitors such as cyclosporin A and FK506 were reported to inhibit synaptic vesicle recycling (Marks and McMahon, 1998). Interestingly, cyclosporin A was also shown to inhibit osteoclast differentiation and bone resorption in culture (Chowdhury et al., 1991; Orcel et al., 1991; Klein et al., 1997). Based on our findings implicating dynamin in podosome function, we tested whether inhibitors of calcineurin disrupts podosomes. Treatment of mouse osteoclasts for 20 min with cyclosporin A resulted in a disruption of their morphology (Fig. 7). Cyclosporin A–treated osteoclasts resembled osteoclasts from $Src^{+/+}$ mice that lack a peripheral ring of podosomes and have decreased motility (Neff et al., 1997). A similar disruption of podosomes was produced by cyclosporin A in Src-transformed fibroblasts (not shown). These results may underlie the reported inhibitory effect of calcineurin antagonists on bone resorp-

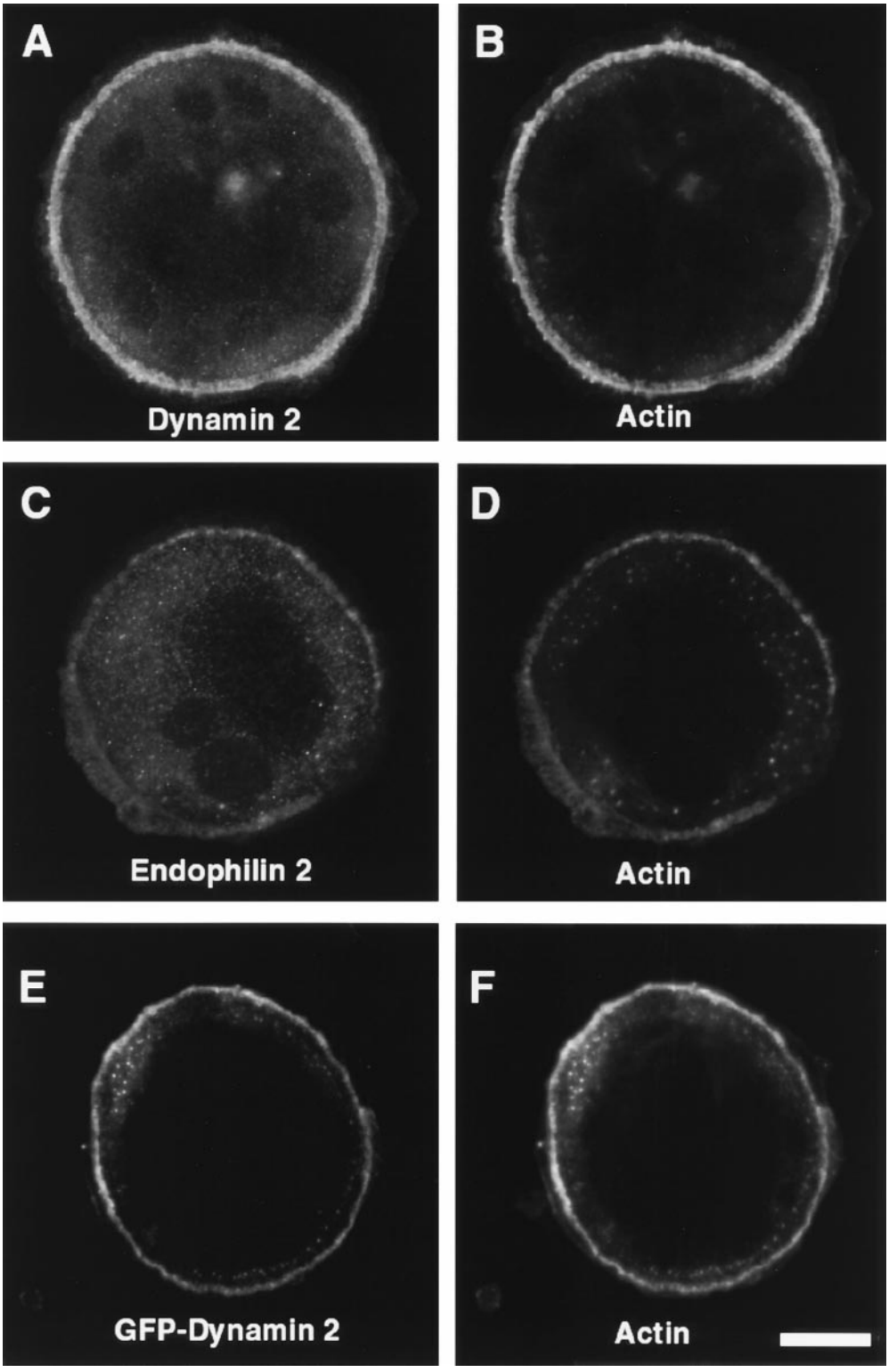

Figure 6. Immunolocalization of dynamin 2 and endophilin 2 in the podosomes of osteoclasts. (A–D) Mouse osteoclasts were immunostained for dynamin 2 and counterstained for actin with phalloidin. All three proteins colocalize in the peripheral sealing zone known to be enriched in podosomes. (E and F) The cDNA encoding GFP-dynamin 2aa was microinjected in the nuclei of the osteoclast. After 6 h, cells were fixed and counterstained for actin with phalloidin. Bar, 42 μM.

tion (Chowdhury et al., 1991; Orcel et al., 1991; Klein et al., 1997).

Disruption of Podosomes by a Temperature-sensitive GFP-Dynamin 2aa Mutant

Studies of dynamin 1 have defined mutations that impair its function and that have a dominant negative effect on endocytosis (Herskovits et al., 1993; van der Bliek et al., 1993; Damke et al., 1994, 1995). A Gly to Asp mutation at position 266 of *Drosophila* dynamin is responsible for the temperature-sensitive phenotype of the *shibire* mutant. A dynamin 1 mutant harboring the analogous mutation was shown to be functional at 30°C but to have a dominant negative effect at 38°C (Damke et al., 1995). A corresponding mutation was introduced in GFP-tagged dy-

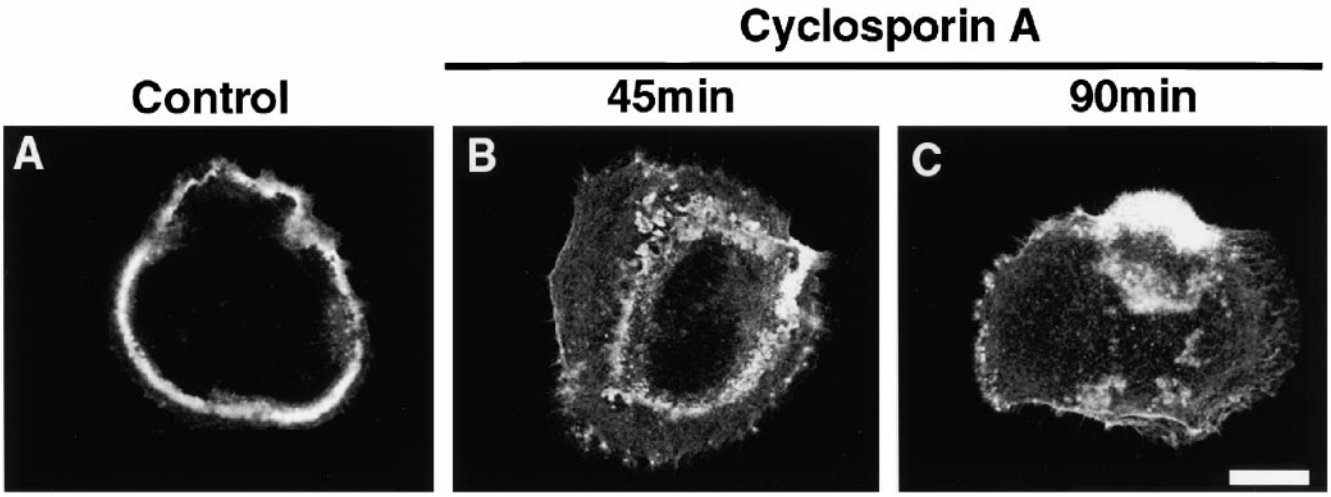

Figure 7. Treatment of osteoclasts with the calcineurin inhibitor cyclosporin A has disruptive affect on podosomes. Phalloidin staining revealing the progressive disruption of podosomes in osteoclasts which were treated with 20 μM cyclosporin A for either 45 (B) or 90 min (C), as compared with a nontreated osteoclast (A). Bar, 70 μM.

namin 2aa (Gly to Asp mutation at position 273) and its effect was tested by transient expression in RSV-transformed BHK21 cells or in v-Src–transformed Balb/c 3T3 cells. At 30°C this mutant localized at podosomes but did not affect their structure (Fig. 8, C and D). In contrast, podosomes were only seldomly observed in transfected cells maintained at 38°C for 12 h after transfection (Fig. 8, A and B). Neighboring untransfected cells had normal podosomes indicating that mutant dynamin, and not the temperature shift was responsible for podosome disappearance. A morphometric analysis revealed that 98 of 100 transfected Balb 3T3 cells had podosomes at the 30°C, but 7 of 100 cells had podosomes at 38°C. In the few cells containing podosomes at this temperature, GFP-dynamin $2aa^{G273D}$ was still localized at podosomes.

We also tested whether another well characterized dominant negative mutation of dynamin 1, the K44A mutation (Herskovits et al., 1993; Damke et al., 1994), had a similar effect on podosomes if introduced into dynamin 2aa. Based on studies of the Ras GTPase, this mutation inhibits GTP binding and hydrolysis. GFP-dynamin $2aa^{K44A}$ was targeted to podosomes but did not disrupt their structure (Fig. 8, E and F). Therefore, we explored the possibility that the K44A mutation may affect functional properties of dynamin 2aa at podosomes not resulting in an obvious modification of their structure.

We used fluorescence recovery after photobleaching (FRAP; Denk et al., 1990; Yuste and Denk, 1995; Xu et al., 1996) to determine the turnover of GFP-actin at podosomes, which are thought to be highly dynamic structures relative to focal adhesion plaques. RSV-transformed BHK21 cells were transfected with GFP-actin and examined by time-lapse two-photon excitation microscopy. After photobleaching, fluorescence nearly recovered within 60 s (Fig. 9, A and B). Jaspakinolide, a potent membrane permeant stabilizer of actin filaments (Bubb et al., 1994), completely abolished the recovery of fluorescence indicating that such recovery is a result of actin dynamics (Fig. 9 C). The FRAP of wild-type GFP-dynamin 2aa had a time course similar to that of actin (Fig. 9 D) and also did not recover in the presence of jasplakinolide (not shown). The rate constants of the recoveries of GFP-actin and GFP-dynamin 2aa were not statistically different ($P = 0.187$) and were 1.89 ± 141 min^{-1} and 1.89 ± 0.236 min^{-1}, respectively. In contrast, GFP-dynamin $2aa^{K44A}$ exhibited a slower recovery (Fig. 9, E and F) with a rate constant of 0.55 ± 057 min^{-1}. Based on these findings we investigated whether dynamin $2aa^{K44A}$ has an effect on the recovery rate of actin, as expected if this mutant dynamin delays actin turnover. FRAP analysis was performed on RSV-transformed BHK21 cells which had been comicroinjected with GFP-actin and a dynamin $2aa^{K44A}$ lacking the GFP-tag. In these cells, GFP-actin had a slower recovery than in control cells with an average rate constant of 1.05 ± 126 min^{-1} (Fig. 9, F and G). This was a statistically significant reduction as compared with the rate constant of recovery observed with GFP-actin alone ($P = 0.02$).

Presence of an Actin Sheath around Dynamin 1–Coated Tubules In Vitro

The working hypothesis of this study, i.e., the possible presence of dynamin at tubular membranes of podosomes, had been triggered by the similarity of these tubules to the dynamin coated tubules visible on cell membranes incubated with ATP and GTPγS (Takei et al., 1995; see also Fig. 2, F–H). Based on the close spatial relationship between actin and dynamin observed at podosomes, we reexamined synaptic membranes incubated with brain cytosol, ATP and GTPγS for the possible presence of analogous structural relationship between the actin cytomatrix and dynamin. As previously reported, dynamin coated tubules, which are also positive for endophilin (Ringstad et al., 1999) are very abundant in this material (Takei et al., 1995). Strikingly, these tubules were not randomly dispersed

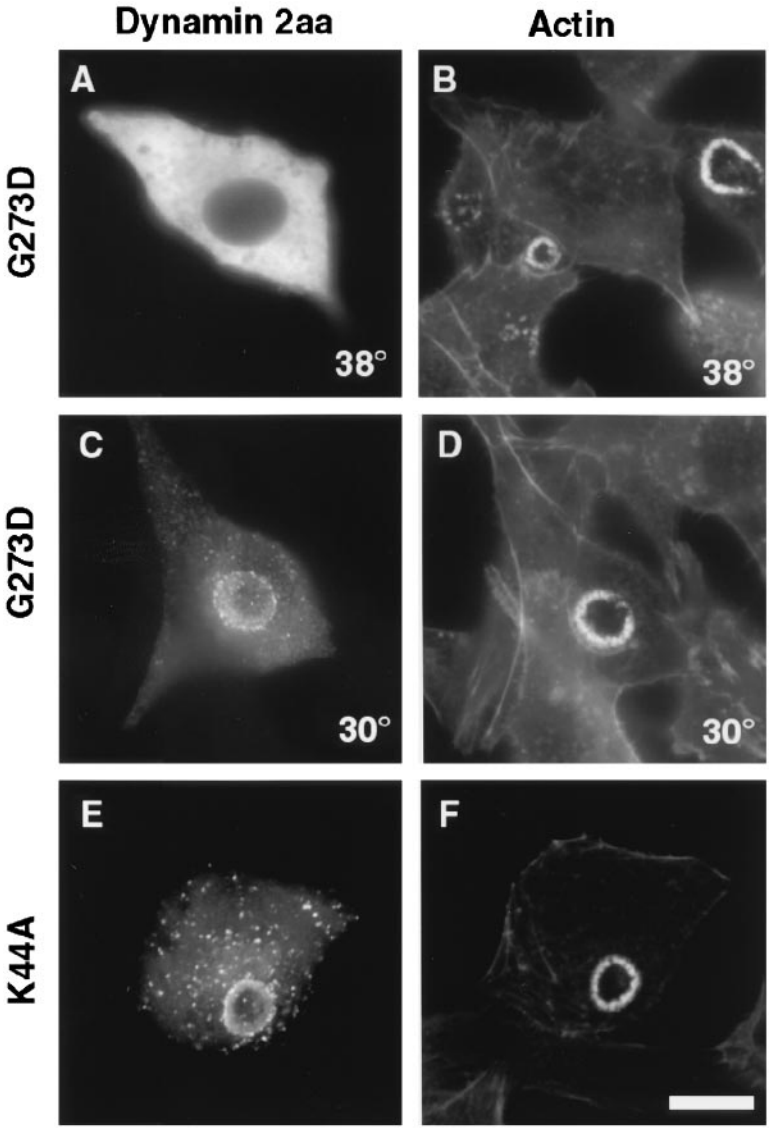

Figure 8. Expression of dynamin $2aa^{G273D}$ and dynamin $2aa^{K44A}$ in transformed BHK21 cells. RSV-transformed BHK21 cells were transiently transfected with GFP-dynamin $2aa^{G273D}$ or with GFP-dynamin $2aa^{K44A}$ as indicated. After transfection cells were kept at either 30°C or 38°C as also indicated. In the cells kept at 38°C no podosomes are present. GFP-dynamin $2aa^{K44A}$ is targeted to the podosome rosettes. All cells were counterstained for actin with phalloidin. Bar, 14 μM.

among other organelles. Instead, they were frequently surrounded by a cytoskeletal matrix and they appeared to represent the core of such matrix, thus generating structures very reminiscent of podosomes in situ (Fig. 2, F and G; see also Ringstad et al., 1999). The presence of actin in this matrix was confirmed by immunogold labeling (Fig. 2 H).

Discussion

Our results reveal a structural and functional link between a pool of dynamin and actin. They demonstrate that dynamin 2aa is a component of the sheath that surrounds the tubular invaginations of the plasma membrane of podosomes. This sheath was previously shown to be composed of a dense actin cytoskeleton containing a variety of actin binding proteins (Tarone et al., 1985; Marchisio et al., 1988; Nermut et al., 1991; Hiura et al., 1995). Thus, our results are convergent with those of recent studies reporting that dynamin directly binds regulatory components of the actin cytoskeleton, such as profilin (Witke et al., 1998), proteins of the syndapin/pacsin/FAP52 family (Merilainen et al., 1997; Qualmann et al., 1999; Ritter et al., 1999), and cortactin (McNiven, M., unpublished observation). The previous link of syndapin/pacsin to dynamin is of special interest because of the localization of a member of this protein family, FAP52, at another actin attachment site, the focal adhesion plaque (Merilainen et al., 1997). Podosomes are present in cells with high levels of motility, Src activity, or both (Tarone et al., 1985; Tanaka et al., 1996). Since dynamin binds Src (Gout et al., 1993; Foster-Barber and Bishop, 1998) and can be a substrate for Src (Ahn et al., 1999), their partnership is likely to be important in podosome function.

Podosomes are highly dynamic structures, even when they cluster in organized arrays, such as in the rosettes of RSV-transformed BHK21 cells and in the peripheral region of osteoclasts. The fast and similar recoveries after photobleaching of GFP-actin and GFP-dynamin 2aa demonstrate that the cytoskeletal meshwork surrounding the central tubule undergoes very rapid turnover. This fast turnover is consistent with the function of podosomes as transient attachment sites in migrating cells such as leuko-

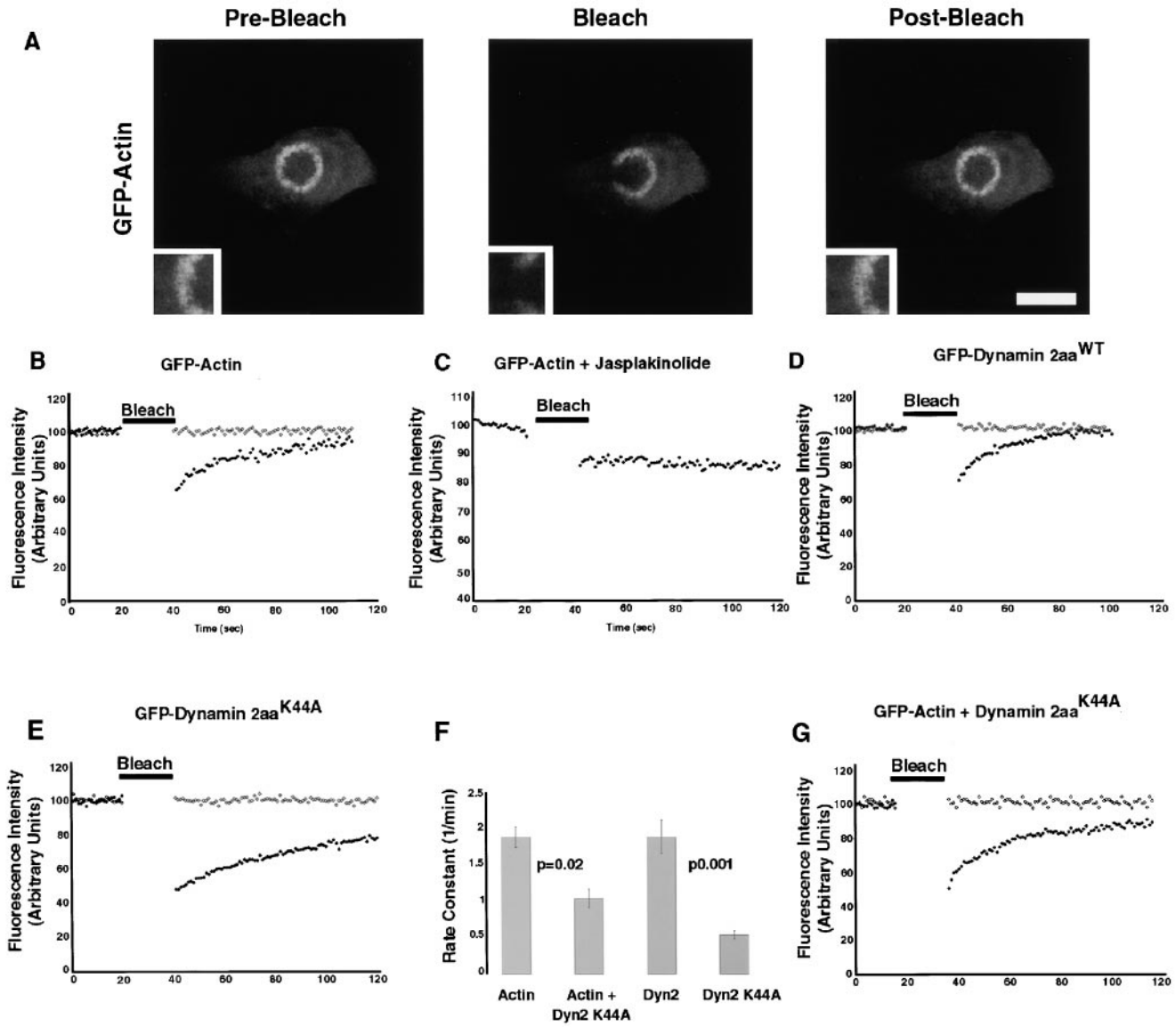

Figure 9. Fluorescence recovery after photobleaching (FRAP) of GFP-actin and GFP-dynamin. RSV-transformed BHK21 cells were transiently transfected with GFP-actin or GFP-dynamin, then bleached for 20 s, and allowed to recover. (A) Micrographs of GFP-actin appearance before bleaching, immediately after bleach, and 1 min post-bleach. (B) Time course of GFP-actin fluorescence in the section of the rosette subjected to photobleaching (closed diamonds) and in a nonbleached region (open diamonds). Fluorescence fully recovered after 60 s with a rate constant of 1.89 ± 1.41 min^{-1} (r^2 = 0.881 ± 0.99). (C) Same as B in the presence of jasplakinolide (1 μM). No recovery occurs in the presence of this drug. (D–F) GFP-dynamin 2aa recovered at a rate very similar to that of GFP-actin, while GFP-dynamin $2aa^{K44A}$ recovered at a much slower rate. E shows the rate constants for GFP-dynamin (k = 1.89 ± 0.236 min^{-1}, r^2 = 0.845 ± 0.01) and GFP-dynamin $2aa^{K44A}$ (k = 0.55 ± 0.57 min^{-1}, r^2 = 0.969 ± 01) and illustrates the statistically significant difference between the two rates. Bar, 14 μM.

cytes (Wolosewick, 1984) and macrophages (Linder et al., 1999). It is also consistent with the presence at podosomes of WASP (Linder et al., 1999), a key regulator of actin dynamics via its action on the Arp2/3 complex (Rohatgi et al., 1999). An attractive possibility is that dynamin may play a role in the dynamics of podosomes, as suggested by our analysis of dynamin 2aa mutants. GFP-dynamin $2aa^{K44A}$ had a slower recovery after photobleaching than wild-type GFP-dynamin 2aa and dynamin $2aa^{K44A}$ delayed actin dynamics. Furthermore, GFP-dynamin $2aa^{G273D}$ disrupted podosomes at the restrictive temperature of 38°C, but not at 30°C. The different effects of the two dynamin mutations may be dependent upon their different effect on factors downstream to dynamin. For example, the GFP-dynamin $2aa^{G273D}$ mutant, but not the GFP-dynamin $2aa^{K44A}$ mutant, may sequester some factor(s) crucial for the formation of podosomes.

Podosomes do not have a direct structural relationship to clathrin coated pits or caveolae and are not thought to have an endocytic function. Thus, our finding extends the

role of dynamin to processes beyond receptor-mediated endocytosis. We note, however, that narrow membrane tubules connecting clathrin-coated pits to the cell surface have been observed in a variety of cell types and experimental conditions. These tubules are surrounded by a cytoskeletal sheath, reminiscent of the one observed at podosomes (Willingham and Pastan, 1983). Furthermore, it cannot be excluded that membrane may flow through the core of podosomes and that vesicles, non clathrin coated, may pinch off at their tips (Fig. 10 A).

Tubular plasma membrane invaginations which are surrounded by an actin cytomatrix and are very similar to podosomes, albeit generally much shorter, are present in yeast. They represent the core of the so-called actin patches which some studies have suggested to be sites of endocytosis (Fig. 10 A; Mulholland et al., 1994). Besides actin, many other yeast actin binding proteins are present in yeast actin patches and many of the mammalian homologues of these proteins are present at podosomes (Balguerie et al., 1999). Such proteins include Sla2 (Yang et al., 1999), Bee1/Las17 (Li, 1997), Sac6 (Adams et al., 1991), and their mammalian homologues talin (Marchisio et al., 1988), WASP (Linder et al., 1999), and fimbrin (Babb et al., 1997), respectively. No dynamin-like proteins have been localized at yeast actin patches so far. It should be noted, however, that dynamin is not the only protein which can generate membrane tubules. The dynamin-interacting protein amphiphysin, for example, is as potent as dynamin in tubule generation (Takei et al., 1999). We note that the yeast protein Rvs167, a homologue of amphiphysin, was recently reported to be localized, and to be functionally important, at yeast actin patches (Balguerie et al., 1999).

Our study provides evidence for a role of dynamin besides the more conventional role of this protein in vesicle fission during receptor-mediated endocytosis (Herskovits et al., 1993; van der Bliek et al., 1993; Henley et al., 1998; Oh et al., 1998). A role of actin in endocytosis is suggested by a variety of studies (Lamaze and Schmid, 1995; Munn et al., 1995; Wendland and Emr, 1998) and recent findings have suggested the presence of a cytoskeletal scaffold which determines sites at which clathrin coated pits form (Gaidarov et al., 1999). As we have shown in Fig. 2, G and H, a sheath of actin-like cytoskeleton can be observed around dynamin coated tubular membranes generated in vitro on synaptic membranes and the link between actin and dynamin suggested by our study may also apply to dynamin isoforms implicated in endocytosis. A pool of actin may be present physiologically around clathrin coated pits, but may be very small and/or transient and therefore difficult to visualize (Fig. 10 B). Thus, the unique organization of actin at podosomes may have revealed a connection between actin and dynamin which applies to other dynamin family members as well, but which is more difficult to demonstrate for dynamin 1 at clathrin coated pits. An important question which remains to be addressed is the precise role of actin in the endocytic reaction of clathrin coated vesicles. Actin may assist fission of the vesicle bud by constricting its neck via an actin-myosin-based mechanisms or by propelling the coated bud away from the plasma membrane via a polarized polymerization-depolymerization cycle, such as the one which propels *Listeria* and *Shigella* within the cytoplasm (Loisel et al., 1999). A direct role of comet-like actin polymerization in the separation of endocytic vesicles from the plasma membrane (Fig. 10 B) was recently suggested by a study of pinocytic vesicles in mast cells (Merrifield et al., 1999). In conclusion, the results of this study suggest a function for a dynamin isoform at actin attachment sites and, conversely, strengthen a putative role of actin in endocytosis.

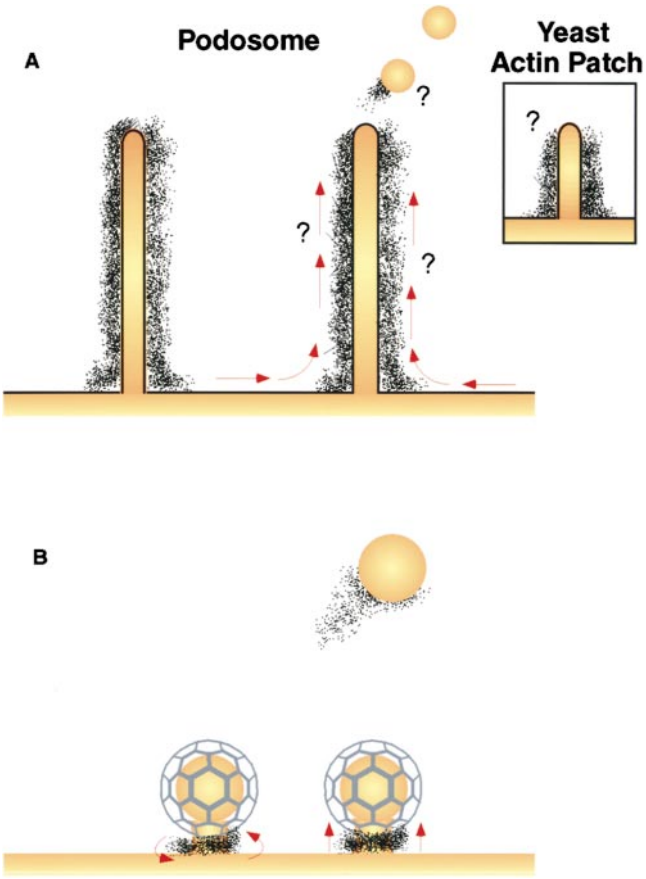

Figure 10. Schematic representation of podosomes and of potential roles of actin in endocytosis. (A) Podosomes (Nitsch et al., 1989), which are represented by columnar arrays of actin enclosing a very narrow tubular invagination of the plasma membrane, have a structure very similar to that previously described for yeast actin patches (inset; Mulholland et al., 1994). The drawing on the right depicts the hypothesis that membrane may flow in the tubular invaginations and that endocytic vesicles may pinch off from their ends. (B) Drawing illustrating the possibility that a cytoskeletal scaffold at the neck of clathrin coated pits may resemble the scaffold surrounding the tubular invagination of podosomes. This scaffold could assist the fission reaction by twisting the neck (left) or by pushing away form the plasma membrane (right). The residual scaffold at the point of fission may drive the formation of actin comets.

We thank Dr. M. Way for the kind gift of GFP-actin; Dr. M. Nathanson and P. Male (Yale, New Haven, CT) for assistance with experiments involving two photon microscopy and FRAP; Dr. O. Cremona (Novara) and Dr. P.C. Marchisio (San Raffaele Scientific Institute, Milano) for discussion; and Drs. U. Maya, A. Lee, W. Garrett, Y. Nemoto, and M. Butler for helpful suggestions.

This work was supported in part by grants from the National Institutes of Health (NS36251 and CA46128 to P. De Camilli and AR42927 to R.

Baron) and by a grant from the United States Army Medical Research and Development Command (to P. De Camilli).

Submitted: 29 December 1999
Revised: 1 June 2000
Accepted: 14 June 2000

References

Adams, A.E., D. Botstein, and D.G. Drubin. 1991. Requirement of yeast fimbrin for actin organization and morphogenesis in vivo. *Nature*. 354:404–408.

Ahn, S., S. Maudsley, L.M. Luttrell, R.J. Lefkowitz, and Y. Daaka. 1999. Src-mediated tyrosine phosphorylation of dynamin is required for beta2-adrenergic receptor internalization and mitogen-activated protein kinase signaling. *J. Biol. Chem*. 274:1185–1188.

Ali, N.N., A. Boyde, and S.J. Jones. 1984. Motility and resorption: osteoclastic activity *in vitro*. *Anat. Embryol. (Ber)*. 170:51–56.

Babb, S.G., P. Matsudaira, M. Sato, I. Correia, and S.S. Lim. 1997. Fimbrin in podosomes of monocyte-derived osteoclasts. *Cell Motil. Cytoskelet.* 37: 308–325.

Balguerie, A., P. Sivadon, M. Bonneu, and M. Aigle. 1999. Rvs167p, the budding yeast homolog of amphiphysin, colocalizes with actin patches. *J. Cell Sci.* 112:2529–2537.

Bauerfeind, R., K. Takei, and P. De Camilli. 1997. Amphiphysin I is associated with coated endocytic intermediates and undergoes stimulation-dependent dephosphorylation in nerve terminals. *J. Biol. Chem*. 272:30984–30992.

Bubb, M.R., A.M. Senderowicz, E.A. Sausville, K.L. Duncan, and E.D. Korn. 1994. Jasplakinolide, a cytotoxic natural product, induces actin polymerization and competitively inhibits the binding of phalloidin to F-actin. *J. Biol. Chem*. 269:14869–14871.

Cameron, P.L., T.C. Sudhof, R. Jahn, and P. De Camilli. 1991. Colocalization of synaptophysin with transferrin receptors: implications for synaptic vesicle biogenesis. *J. Cell Biol.* 115:151–164.

Cao, H., F. Garcia, and M.A. McNiven. 1998. Differential distribution of dynamin isoforms in mammalian cells. *Mol. Biol. Cell.* 9:2595–2609.

Chambers, T.J., and C.J. Mangus. 1982. Calcitonin alters behavior of isolated osteoclasts. *J. Pathol.* 136:27–39.

Chen, M.S., R.A. Obar, C.C. Schroeder, T.W. Austin, C.A. Poodry, S.C. Wadsworth, and R.B. Vallee. 1991. Multiple forms of dynamin are encoded by shibire, a *Drosophila* gene involved in endocytosis. *Nature*. 351:583–586.

Chowdhury, M.H., V. Shen, and D.W. Dempster. 1991. Effects of cyclosporine A on chick osteoclasts in vitro. *Calcif. Tissue Int.* 49:275–279.

Damke, H., T. Baba, D.E. Warnock, and S.L. Schmid. 1994. Induction of mutant dynamin specifically blocks endocytic coated vesicle formation. *J. Cell Biol*. 127:915–934.

Damke, H., M. Gossen, S. Freundlieb, H. Bujard, and S.L. Schmid. 1995. Tightly regulated and inducible expression of dominant interfering dynamin mutant in stably transformed HeLa cells. *Methods Enzymol.* 257:209–220.

De Camilli, P., and K. Takei. 1996. Molecular mechanisms in synaptic vesicle endocytosis and recycling. *Neuron*. 16:481–486.

DeFife, K.M., C.R. Jenney, E. Colton, and J.M. Anderson. 1999. Cytoskeletal and adhesive structural polarizations accompany IL-13-induced human macrophage fusion. *J. Histochem. Cytochem*. 47:65–74.

Denk, W., J.H. Strickler, and W.W. Webb. 1990. Two-photon laser scanning fluorescence microscopy. *Science*. 248:73–76.

Foster-Barber, A., and J.M. Bishop. 1998. Src interacts with dynamin and synapsin in neuronal cells. *Proc. Natl. Acad. Sci. USA*. 95:4673–4677.

Gaidarov, I., F. Santini, R.A. Warren, and J.H. Keen. 1999. Spatial control of coated-pit dynamics in living cells. *Nat. Cell Biol.* 1:1–7.

Gavazzi, I., M.V. Nermut, and P.C. Marchisio. 1989. Ultrastructure and gold-immunolabeling of cell-substratum adhesions (podosomes) in RSV-transformed BHK cells. *J. Cell Sci.* 94:85–99.

Gold, E.S., D.M. Underhill, N.S. Morrissette, J. Guo, M.A. McNiven, and A. Aderem. 1999. Dynamin 2 is required for phagocytosis macrophages. *J. Exp. Med*. 190:1849–1856.

Gout, I., R. Dhand, I.D. Hiles, M.J. Fry, G. Panayotou, P. Das, O. Truong, N.F. Totty, J. Hsuan, G.W. Booker, I.D. Campbell, and M.D. Waterfield. 1993. The GTPase dynamin binds to and is activated by a subset of SH3 domains. *Cell*. 75:25–36.

Henley, J.R., E.W.A. Krueger, B.J. Oswald, and M.A. McNiven. 1998. Dynamin-mediated internalization of caveolae. *J. Cell Biol.* 141:85–99.

Herskovits, J.S., C.C. Burgess, R.A. Obar, and R.B. Vallee. 1993. Effects of mutant rat dynamin on endocytosis. *J. Cell Biol.* 122:565–578.

Hinshaw, J.E., and S.L. Schmid. 1995. Dynamin self-assembles into rings suggesting a mechanism for coated vesicle budding. *Nature*. 374:190–192.

Hiura, K., S.S. Lim, S.P. Little, S. Lin, and M. Sato. 1995. Differentiation dependent expression of tensin and cortactin in chicken osteoclasts. *Cell Motil. Cytoskelet.* 30:272–284.

Horne, W.C., L. Neff, D. Chatterjee, A. Lomri, J.B. Levy, and R. Baron. 1992. Osteoclasts express high levels of pp60c-src in association with intracellular membranes. *J. Cell Biol.* 119:1003–1013.

Jones, S.M., K.E. Howell, J.R. Henley, H. Cao, and M.A. McNiven. 1998. Role of dynamin in the formation of transport vesicles from the trans-Golgi network. *Science*. 279:573–577.

Klein, B.Y., I. Gal, R. Mosheiff, M. Liebergall, and H. Ben-Bassat. 1997. Cyclosporin A and its non-immunosuppressive derivative exhibit a differential effect on cell-mediated mineralization in culture. *J. Cell Biochem*. 64:209–216.

Koenig, J.H., and K. Ikeda. 1983. Evidence for a presynaptic blockage of transmission in a temperature-sensitive mutant of *Drosophila*. *J. Neurobiol.* 14: 411–419.

Koenig, J.H., and K. Ikeda. 1989. Disappearance and reformation of synaptic vesicle membrane upon transmitter release observed under reversible blockage of membrane retrieval. *J. Neurosci.* 9:3844–3860.

Lai, M.M., J.J. Hong, A.M. Ruggiero, P.E. Burnett, V.I. Slepnev, P. De Camilli, and S.H. Snyder. 1999. The calcineurin-dynamin 1 complex as a calcium sensor for synaptic vesicle endocytosis. *J. Biol. Chem*. 274:25963–25966.

Lamaze, C., and S.L. Schmid. 1995. The emergence of clathrin-independent pinocytic pathways. *Curr. Opin. Cell Biol.* 7:573–580.

Lamaze, C., L.M. Fujimoto, H.L. Yin, and S.L. Schmid. 1997. The actin cytoskeleton is required for receptor-mediated endocytosis in mammalian cells. *J. Biol. Chem*. 272:20332–20335.

Li, R. 1997. Bee1, a yeast protein with homology to Wiscott-Aldrich syndrome protein, is critical for the assembly of cortical actin cytoskeleton. *J. Cell Biol.* 136:649–658.

Linder, S., D. Nelson, M. Weiss, and M. Aepfelbacher. 1999. Wiskott-Aldrich syndrome protein regulates podosomes in primary human macrophages. *Proc. Natl. Acad. Sci. USA*. 96:9648–9653.

Liu, J.P., A.T. Sim, and P.J. Robinson. 1994. Calcineurin inhibition of dynamin I GTPase activity coupled to nerve terminal depolarization. *Science*. 265: 970–973.

Loisel, T.P., R. Boujemaa, D. Pantaloni, and M.F. Carlier. 1999. Reconstitution of actin-based motility of Listeria and Shigella using pure proteins. *Nature*. 401:613–616.

Marchisio, P.C., L. Bergui, G.C. Corbascio, O. Cremona, N. D'Urso, M. Schena, L. Tesio, and F. Caligaris-Cappio. 1988. Vinculin, talin, and integrins are localized at specific adhesion sites of malignant B lymphocytes. *Blood*. 72:830–833.

Marks, B., and H.T. McMahon. 1998. Calcium triggers calcineurin-dependent synaptic vesicle recycling in mammalian nerve terminals. *Curr. Biol.* 8:740–749.

Merilainen, J., V.P. Lehto, and V.M. Wasenius. 1997. FAP52, a novel, SH3 domain-containing focal adhesion protein. *J. Biol. Chem*. 272:23278–23284.

Merrifield, C.J., S.E. Stephen E. Moss, C. Ballestrem, B.A. Imhof, G. Giese, I. Wunderlich, and W. Almers. 1999. Endocytic vesicles move at the tips of actin tails in cultured mast cells. *Nat. Cell Biol.* 1:72–74.

Mulholland, J., D. Preuss, A. Moon, A. Wong, D. Drubin, and D. Botstein. 1994. Ultrastructure of the yeast actin cytoskeleton and its association with the plasma membrane. *J. Cell Biol.* 125:381–391.

Mundigl, O., G.C. Ochoa, C. David, V.I. Slepnev, A. Kabanov, and P. De Camilli. 1998. Amphiphysin I antisense oligonucleotides inhibit neurite outgrowth in cultured hippocampal neurons. *J. Neurosci.* 18:93–103.

Munn, A.L., B.J. Stevenson, M.I. Geli, and H. Riezman. 1995. end5, end6, and end7: mutations that cause actin delocalization and block the internalization step of endocytosis in *Saccharomyces cerevisiae*. *Mol. Biol. Cell.* 6:1721–1742.

Neff, L., C. Bardelay, M. Amling, E. Antoine, M. Smadja, D. Brugere, L. Lepescheux, P. Hunt, M. Gaillard-Kelly, J. Levy, and R. Baron. 1997. Decreased motility of the peripheral cytoskeleton and total cell mobility in c-Src-deficient osteoclasts. *J. Bone Miner. Res.* 12(Suppl.):S419.

Nermut, M.V., P. Eason, E.M. Hirst, and S. Kellie. 1991. Cell/substratum adhesions in RSV-transformed rat fibroblasts. *Exp. Cell Res.* 193:382–397.

Nitsch, L., E. Gionti, R. Cancedda, and P.C. Marchisio. 1989. The podosomes of Rous sarcoma virus transformed chondrocytes show a peculiar ultrastructural organization. *Cell Biol. Int. Rep.* 13:919–926.

Oh, P., D.P. McIntosh, and J.E. Schnitzer. 1998. Dynamin at the neck of caveolae mediates their budding to form transport vesicles by GTP-driven fission from the plasma membrane of endothelium. *J. Cell Biol.* 141:101–114.

Orcel, P., M.A. Denne, and M.C. de Vernejoul. 1991. Cyclosporin-A in vitro decreases bone resorption, osteoclast formation, and the fusion of cells of the monocyte-macrophage lineage. *Endocrinology*. 128:1638–1646.

Qualmann, B., J. Roos, P.J. DiGregorio, and R.B. Kelly. 1999. Syndapin I, a synaptic dynamin-binding protein that associates with the neural Wiskott-Aldrich syndrome protein. *Mol. Biol. Cell.* 10:501–513.

Ringstad, N., Y. Nemoto, and P. De Camilli. 1997. The SH3p4/Sh3p8/SH3p13 protein family: binding partners for synaptojanin and dynamin via a Grb2-like Src homology 3 domain. *Proc. Natl. Acad. Sci. USA*. 94:8569–8574.

Ringstad, N., H. Gad, P. Löw, G. Di Paolo, L. Brodin, O. Shupliakov, and P. De Camilli. 1999. Endophilin/SH3p4 is required for the transition from early to late stages in clathrin-mediated synaptic vesicle endocytosis. *Neuron*. 24: 143–154.

Ritter, B., J. Modregger, M. Paulsson, and M. Plomann. 1999. PACSIN 2, a novel member of the PACSIN family of cytoplasmic adapter proteins. *FEBS Lett*. 454:356–362.

Rohatgi, R., L. Ma, H. Miki, M. Lopez, T. Kirchhausen, T. Takenawa, and M.W. Kirschner. 1999. The interaction between N-WASP and the Arp2/3 complex links Cdc42-dependent signals to actin assembly. *Cell*. 97:221–231.

Roos, J., and R.B. Kelly. 1997. Is dynamin really a 'pinchase'? *Trends Cell Biol.* 7:257–259.

Schmid, S.L., M.A. McNiven, and P. De Camilli. 1998. Dynamin and its part-

ners: a progress report. *Curr. Opin. Cell Biol.* 10:504–512.
Schmidt, A., M. Wolde, C. Thiele, W. Fest, H. Kratzin, A.V. Podtelejnikov, W. Witke, W.B. Huttner, and H.D. Soling. 1999. Endophilin I mediates synaptic vesicle formation by transfer of arachidonate to lysophosphatidic acid. *Nature*. 401:133–141.
Schnitzer, J.E., P. Oh, and D.P. McIntosh. 1996. Role of GTP hydrolysis in fission of caveolae directly from plasma membranes. *Science*. 274:239–242.
Sever, S., A.B. Muhlberg, and S.L. Schmid. 1999. Impairment of dynamin's GAP domain stimulates receptor-mediated endocytosis. *Nature*. 398:481–486.
Slepnev, V.I., G.C. Ochoa, M.H. Butler, D. Grabs, and P.D. Camilli. 1998. Role of phosphorylation in regulation of the assembly of endocytic coat complexes. *Science*. 281:821–824.
Sontag, J.M., E.M. Fykse, Y. Ushkaryov, J.P. Liu, P.J. Robinson, and T.C. Südhof. 1994. Differential expression and regulation of multiple dynamins. *J. Biol. Chem*. 269:4547–4554.
Soriano, P., C. Montgomery, R. Geske, and A. Bradley. 1991. Targeted disruption of the c-src proto-oncogene leads to osteopetrosis in mice. *Cell*. 64:693–702.
Sparks, A.B., N.G. Hoffman, S.J. McConnell, D.M. Fowlkes, and B.K. Kay. 1996. Cloning of ligand targets. *Nat. Biotechnol.* 14:741–744.
Sweitzer, S.M., and J.E. Hinshaw. 1998. Dynamin undergoes a GTP-dependent conformational change causing vesiculation. *Cell*. 93:1021–1029.
Takei, K., P.S. McPherson, S.L. Schmid, and P. De Camilli. 1995. Tubular membrane invaginations coated by dynamin rings are induced by GTPγS in nerve terminals. *Nature*. 374:186–190.
Takei, K., V. Haucke, V. Slepnev, K. Farsad, M. Salazar, H. Chen, and P. De Camilli. 1998. Generation of coated intermediates of clathrin-mediated endocytosis on protein-free liposomes. *Cell*. 94:131–141.
Takei, K., V.I. Slepnev, V. Haucke, and P. De Camilli. 1999. Functional partnership between amphiphysin and dynamin in clathrin-mediated endocytosis. *Nat. Cell Biol.* 1:33–39.
Tanaka, S., M. Amling, L. Neff, A. Peyman, E. Uhlmann, J.B. Levy, and R. Baron. 1996. c-Cbl is downstream of c-Src in a signalling pathway necessary for bone resorption. *Nature*. 383:528–531.
Tarone, G., D. Cirillo, F.G. Giancotti, P.M. Comoglio, and P.C. Marchisio. 1985. Rous sarcoma virus-transformed fibroblasts adhere primarily at discrete protrusions of the ventral membrane called podosomes. *Exp. Cell Res.* 159:141–157.
Thomas, S.M., and J.S. Brugge. 1997. Cellular functions regulated by Src family kinases. *Annu. Rev. Cell Dev. Biol.* 13:513–609.
Torre, E., M.A. McNiven, and R. Urrutia. 1994. Dynamin 1 antisense oligonucleotide treatment prevents neurite formation in cultured hippocampal neurons. *J. Biol. Chem*. 269:32411–32417.
Urrutia, R., J.R. Henley, T. Cook, and M.A. McNiven. 1997. The dynamins: redundant or distinct functions for an expanding family of related GTPases? *Proc. Natl. Acad. Sci. USA*. 94:377–384.
van der Bliek, A.M., and E.M. Meyerowitz. 1991. Dynamin-like protein encoded by the *Drosophila* shibire gene associated with vesicular traffic. *Nature*. 351:411–414.
van der Bliek, A.M., T.E. Redelmeier, H. Damke, E.J. Tisdale, E.M. Meyerowitz, and S.L. Schmid. 1993. Mutations in human dynamin block an intermediate stage in coated vesicle formation. *J. Cell Biol.* 122:553–563.
Wendland, B., and S.D. Emr. 1998. Pan1p, yeast eps15, functions as a multivalent adaptor that coordinates protein-protein interactions essential for endocytosis. *J. Cell Biol.* 141:71–84.
Willingham, M.C., and I. Pastan. 1983. Formation of receptosomes from plasma membrane coated pits during endocytosis: analysis by serial sections with improved membrane labeling and preservation techniques. *Proc. Natl. Acad. Sci. USA*. 80:5617–5621.
Witke, W., A.V. Podtelejnikov, A. Di Nardo, J.D. Sutherland, C.B. Gurniak, C. Dotti, and M. Mann. 1998. In mouse brain profilin I and profilin II associate with regulators of the endocytic pathway and actin assembly. *EMBO (Eur. Mol. Biol. Organ.) J.* 17:967–976.
Wolosewick, J.J. 1984. Distribution of actin in migrating leukocytes in vivo. *Cell Tissue Res.* 236:517–525.
Wu, H., and J.T. Parsons. 1993. Cortactin, an 80/85-kilodalton pp60src substrate, is a filamentous actin-binding protein enriched in the cell cortex. *J. Cell Biol.* 120:1417–1426.
Xu, C., W. Zipfel, J.B. Shear, R.M. Williams, and W.W. Webb. 1996. Multiphoton fluorescence excitation: new spectral windows for biological nonlinear microscopy. *Proc. Natl. Acad. Sci. USA*. 93:10763–10768.
Yang, S., M.J. Cope, and D.G. Drubin. 1999. Sla2p is associated with the yeast cortical actin cytoskeleton via redundant localization signals. *Mol. Biol. Cell.* 10:2265–2283.
Yuste, R., and W. Denk. 1995. Dendritic spines as basic functional units of neuronal integration. *Nature*. 375:682–684.
Zambonin-Zallone, A., A. Teti, A. Carano, and P.C. Marchisio. 1988. The distribution of podosomes in osteoclasts cultured on bone laminae: effect of retinol. *J. Bone Miner. Res.* 3:517–523.